COVER SHEET

Superplastic Deformation Behavior of $Zr_{41.25}Ti_{13.75}Ni_{10}Cu_{12.5}Be_{22.5}$ Bulk Metallic Glass in Supercooled Liquid Region

J.F. Sun[a], G. Wang[a,b], J. Shen[a,c,*], Z.H. Stachurski[b], C. Yan[c], L. Ye[c], B.D. Zhou[a]

[a] *School of Materials Science and Engineering, Harbin Institute of Technology, Harbin 150001,China*

[b] *Faculty of Engineering and Information Technology, The Australian National University, Canberra, ACT 0200, Australia*

[c] *School of Aerospace, Mechanical and Mechatronic Engineering, The University of Sydney, NSW 2006, Australia*

Abstract

This paper presents the tensile deformation behavior of $Zr_{41.25}Ti_{13.75}Ni_{10}Cu_{12.5}Be_{22.5}$ bulk metallic glass in supercooled liquid region. Isothermal tensile tests are carried out at four characteristic temperatures of 616K, 636K, 656K and 676K which are in the range from glass transition onset temperature to crystallization temperature. The results show that the superplastic flow behaviors of the material, viz., the flow stress and the elongation, vary depending strongly on the testing temperature and initial strain-rate. At a given temperature, the elongation increases firstly and then decreases with the initial strain-rate increasing, and the maximum elongation is found to be as high as 1625% at the temperature of 656K with the strain-rate $7.6\times10^{-3}s^{-1}$. DSC analysis shows that the crystalline volume fraction of deformed section is always higher than that of undeformed section in the specimens. The maximum elongation always corresponds to the maximum crystalline volume fraction. The nanocrystals homogeneously embedded in the amorphous matrix of the deformed specimens can be observed by using TEM. It is resultantly believed that the presence of amorphous-crystalline duplex phase microstructure has a pronounced effect on the superplastic deformation behavior of the material.

Key words Bulk metallic glass Superplastic deformation Nanocrystallization

* Corresponding author. E-mail address: junshen@public.hr.hl.cn (J. Shen).

1. Introduction

Zr-based bulk metallic glasses have unique mechanical properties such as high strength and low elastic modulus[1, 2]. Meanwhile they have a good processability in the supercooled liquid state, this property should lead to applications in the fields of near-net-shape fabrication of complex structural components[3, 4]. Since 1990's, superplastic behavior of bulk metallic glasses in the supercooled liquid region has been intensively studied by many investigators[5~10]. Kawamura *et al.* studied the high temperature deformation behavior of Zr-based metallic glass and found that the high temperature deformation behavior was classified Newtonian type flow and non-Newtonian type flow. In general, Newtonian flow behavior, which is accompanied by high tensile elongations, indicates the strain-rate hardening mechanism dominating the deformation of amorphous phase. Nieh[11], Lee[12] and Bae[13] *et al.* studied the phase transformation of bulk metallic glass during the superplastic flow process and found that nanocrystallization was induced by stress. Nieh[14] suggested that non-Newtonian type flow can be attributed to nanocrystallization during deformation. In this paper, we attempt to investigate and understand the tensile deformation behavior of a $Zr_{41.2}Ti_{13.8}Cu_{12.5}Ni_{10}Be_{22.5}$ bulk metallic glass for various initial strain rates and temperatures.

2. Experimental Procedure

The material used in the present study has a composition of $Zr_{41.25}Ti_{13.75}Ni_{10}Cu_{12.5}Be_{22.5}$ (at.%). Alloy ingots were prepared by arc-melting mixture of pure metal elements in a titanium-gettered argon atmosphere, followed by suction into copper mold to form 3×70×30mm plate-like alloy samples. Transmission electron microscopy (TEM) was performed using PHILIPS TECNAI 20 type (200KV) transmission electron microscope. The samples for TEM observation were prepared using standard twin-jet electropolishing in a solution containing one part nitric acid plus two parts methanol at –25^{o}C.

The thermal properties of the alloy were measured using differential scanning calorimetry (DSC) in a Pekin-Elmer Pyris 1 DSC. The glass transition onset temperature (T_g^{onset}), glass transition end temperature (T_g^{end}) and crystallization temperature (T_x) are determined to be 616K, 656K and 698K, respectively at a heating rate 20K/min (Fig.1).

Tensile sheet specimens were prepared from the as-cast plates by means of electrical discharge machining. They had a gage length of 11mm, a thickness of 3mm and a width of 1.2mm. Tensile tests were conducted using Instron 5500R1186 type machine equipped with an air furnace. Tensile tests were carried out at the temperatures of 616K, 636K, 656K and 676K, which are in the range of T_g~T_x.

3. Results and Discussion

Fig.2 shows the strain-stress curves of $Zr_{41.25}Ti_{13.75}Ni_{10}Cu_{12.5}Be_{22.5}$ alloy obtained at different temperatures with different initial strain-rates. The amorphous alloy shows homogeneous deformation in supercooled liquid region. Typically the flow stress reaches a peak just after yielding and then decreases significantly with increasing strain. It is readily observed that the levels of yield stress and flow stress decrease with increasing temperature or decreasing strain-rate. This yield drop phenomenon has been reported in $Pd_{40}Ni_{40}P_{20}$[5], $Zr_{65}Al_{10}Ni_{10}Cu_{15}$[7], $Fe_{72}Hf_8Nb_2B_{18}$[8] and $Zr_{52.5}Ti_5Ni_{14.6}Cu_{17.9}Al_{10}$[12] alloys. This phenomenon was interpreted in terms of non-linear viscoelasticity and flow stress producing more free volume. Meantime it is evident in Fig.2 that flow stress, peak stress and elongation depend strongly on the strain-rates and the testing temperatures. At a given temperature, the level of peak stress and flow stress increases with increasing strain-rate. When the strain-rate increases to a limited value, the fracture appears a brittle fracture mode. The elongation increases firstly and then decreases with the velocity increasing and the maximum elongation reaches as high as 1625% at the temperature of 656K with the strain-rate $7.6\times10^{-3}s^{-1}$. Fig.3 shows the photographs of the tensile test specimens at 656K with

differential initial strain-rates.

To further ascertain the microstructure evolution during the superplastic deformation, a series of DSC analysis was carried out on deformed specimens. Although the tensile test temperature is in the supercooled liquid region, it is possible that the strain energy caused by superplastic deformation will complement the thermal energy required for crystallization, as was suggested by Lee[12], Bae[13] and Nieh[14], *et al.* Two samples were prepared from every deformed specimen. One piece was cut from the grip section(undeformed section), and another piece was cut from the region near the fracture point (deformed section). Figs.4~5 show the DSC curves for the pieces cut from the undeformed section and cut from the deformed section after tensile tested at 636K and 656K repspectively. For the purpose of comparison, the DSC curves for the as-cast $Zr_{41.25}Ti_{13.75}Ni_{10}Cu_{12.5}Be_{22.5}$ alloy is also given. The DSC curves for the specimens, which deformed with higher strain-rates, are similar to those of the as-cast specimens, although the heats of crystallization are lower for the former. When the strain-rate decreases to $1.5\times10^{-3}s^{-1}$for 636K, $7.6\times10^{-3}s^{-1}$for 656K and $3\times10^{-2}s^{-1}$ for 676K, the first crystalline peaks on the DSC traces disappear. These results indicate that amorphous phase evolves to a primary crystallization during deformation. All data obtained by the DSC analysis are summarized in Table 1.

As we know, bulk metallic glass generally exhibits a distinct glass transition accompanied by an endothermic reaction (T_g), followed by the appearance of a wide supercooled liquid region ($\Delta T_x=T_x-T_g$), and then an exothermic reaction due to crystallization starting at the crystallization onset temperature (T_x). The amount of heat of crystallization can be obtained by measuring the exothermic crystallization peak area. Using heat of crystallization, the crystalline fraction for deformed specimens can be calculated as follows:

$$V_f = \left(1-\frac{\Delta H_D}{\Delta H_C}\right)\times 100\% \qquad (1)$$

where ΔH_D is the heat of crystallization for a deformed specimen; ΔH_C the heat of crystallization for the as-cast metallic glass.

Fig.6 shows the crystalline fraction and elongation change with the strain-rates at the different temperatures. It is evident that the crystalline fractions of the undeformed sections decrease with the strain-rate increasing, because the time of samples exposed at high temperature increase with the strain-rate decreasing. The crystalline fractions of deformed sections are always higher than the fractions of the undeformed sections. This phenomenon indicates that the amorphous phase transformation is affected by two factors of environmental heating and flow stress. For the undeformed sections, the samples are just affected by isothermal treatment during the superplastic tensile process. But for the deformed sections, the samples are affected by flow stress and isothermal treatment. Lee[12] and Nieh[14] *et al.* studied the microstructure of bulk metallic glass after superplastic deformation and suggested that the flow stress could induce crystallization in bulk metallic glasses at temperature below the crystallization temperature during the superplastic deformation. Indeed, when isothermal annealing is carried out in the supercooled liquid region, amorphous to crystalline phase transformation will occurr. It is the applied flow stress that promotes the phase transformation.

Also as seen in Fig.6, the changes of crystalline fraction of the deformed samples with strain-rate are quite different from those of the undeformed samples. The former generally shows a peak (except deformation at a lower temperature of 616K) at a specific strain-rate, roughly, at which the elongation also features a peak value. For example, in the case of deformation at the temperature of 636K with the strain-rate of $1.5\times10^{-3}s^{-1}$, the elongation of the specimen reaches its maximum of 1110%, and the crystalline fraction reaches its maximum of 42.6%. This implies that, cystallization occurres to a largest extend in the deformation process of the deformed samples with a largest elongation. This phenomenon

provide a direct evidence that crystallization of amorphous material could be activated either by heating of by stress.

Fig.7(a, b) shows the TEM image and the corresponding SAED pattern for the sample which was deformed at 636K with the strain-rate $7.6\times10^{-4}s^{-1}$. Fig.7(c, d) shows the TEM image and the corresponding SAED pattern for the sample which was deformed at 656K with the strain-rate $7.6\times10^{-3}s^{-1}$. The TEM samples were cut from the deformed section. It is evident in fig.7(a) and (b) that some changes of the microstructure occurs. The TEM images show that there are dispersed nanocrystals embedded in the amorphous phase matrix. The nanocrystal sizes are approximately 10±3nm for 636K and 25±3nm for 656K. The corresponding selected-area electron diffraction (SAED) patterns show the polycrystalline halos, because the precipitated phase size is too small. The SAED shown in fig.7(b) displays the multilayer rings which indicate that a substantial fraction of the amorphous phase still exists. Based on the fig.7(d), the nanocrystals are determined to be hexagonal Be_2Zr for the specimens deformed at 656K (Fig.6(c)). This result agrees well with, and could surpass the argument made by Busch[15] and Wanderka[16]. They suggested that $Zr_{41.25}Ti_{13.75}Ni_{10}Cu_{12.5}Be_{22.5}$ metallic glass annealed between 613K and 673K would undergo decomposition and primary crystallization. The decomposition brings out Be-rich region and Zr-rich region. When $Zr_{41.25}Ti_{13.75}Ni_{10}Cu_{12.5}Be_{22.5}$ metallic glass is deformed at 616K, the metastable Zr_2Ni phase precipitates from the decomposition Zr-rich region first. Then, at 656K, the primary crystallization occurs. The Be_2Zr phase as a dominant phase precipitates from the decomposed Be-rich region.

4. Conclusions

(1) The superplastic flow behaviors of $Zr_{41.25}Ti_{13.75}Ni_{10}Cu_{12.5}Be_{22.5}$ bulk metallic glass in the supercooled liquid region, viz., the flow stress and the elongation, vary depending strongly on the

testing temperature and initial strain-rate. The elongation increases firstly and then decreases with the strain-rate increasing and the maximum elongation reaches as high as 1625% at 656K with the strain-rate $7.6\times10^{-3}s^{-1}$.

(2) The crystalline volume fraction of deformed section is always higher than the crystalline fraction of undeformed section of the tensile test specimens. The maximum elongation always corresponds to the maximum crystalline volume fraction. And consequently, flow stress and environmental temperature are believed to be two main factors for affecting the phase transformation during the superplastic deformation of amorphous material.

Reference

[1] Akihisa Inoue. Acta Mater.. 2000, 48: 279.

[2] William L. Johnson. MRS Bulletin. 1999, October.

[3] Yasunori Saotome, Kazuo Itoh, Tao Zhang and Akihisa Inoue. Scripta Mater. 2001, 44: 1541.

[4] Yasunori Saotome, Toshihisa Hatori, Tao Zhang and Akihisa Inoue. Materials Science and Engineering. 2001, A304-306: 716.

[5] Yoshihito Kawamura, Toshihiro Nakamura and Akihisa Inoue. Scripta Mater. 1998, 39(3): 301.

[6] Yoshitito Kawamura, Toshihiro Nakamura, Hidemi Kato, Hideo Mano and Akihisa Inoue. Materials Science and Engineering. 2001, A304-306: 674.

[7] Yoshihito Kawamura, Tsutomu Shibata, Akihisa Inoue and Tsuyoshi Masumoto. Scripta Mater. 1997, 37(4): 431.

[8] Yoshihito Kawamura, Takaomi Itoi, Toshihiro Nakamura and Akihisa Inoue. Materials Science and Engineering. 2001, A304-306: 735.

[9] Hidemi Kato, Yoshihito Kawamura, Akihisa Inoue and Ho-sou Chen. Materials Science and

Engineering. 2001, A304-306: 758.

[10] J.P. Chu, C.L. Chiang, T.G. Nieh and Y. Kawamura. Intermetallic. 2002, 10: 1191.

[11] T.G. Nieh, T. Mukai and C.T. Liu. Scripta Mater. 1999, 40(9): 1021.

[12] Kwang Seok Lee, Tae Kwon Ha, Sangho Ahn and Young Won Chang. Jounal of Non-Crystalline Solids. 2003, 317: 193.

[13] D.H. Bae, H.K. Lim, S.H. Kim, D.H. Kim and W.T. Kim. Acta Materialia. 2002, 50: 1749.

[14] T.G. Nieh, J. Wadsworth, C.T. Liu, T. Ohkubo and Y. Hirotsu. Acta Meter. 2001, 49: 2887.

[15] R. Busch, Y.J. Kim, S. Schneider and W.L. Johnson. Materials Science Forum. 1996, 225-227: 77.

[16] N. Wanderka, Q. Wei, R. Doole, M. Jenkins, S. Friedrich, M.-P. Macht and H. Wollenberger. Materials Science Forum. 1998, 269-272: 773.

Table 1. Elongation and ΔH_D for deformed and undeformed specimens tensile tested under various test conditions

Temperature (K)	Initial strain-rate (s^{-1})	Heating time (s)	Elongation (%)	ΔH_D (J/g) (Undeformed section)	ΔH_D (J/g) (Deformed section)
616	7.6×10^{-4}	2603	197	-89.5	-89.7
	1.5×10^{-3}	892	135	-88.8	-85.4
	3.8×10^{-3}	373	22	-94.9	-94.4
636	7.6×10^{-4}	7999	606	-69.2	-65.3
	1.5×10^{-3}	7326	1110	-81.7	-59.6
	3.8×10^{-3}	428	162	-96.9	-90.0
	7.6×10^{-3}	112	84	-98.6	-93.9
656	1.5×10^{-3}	6234	945	-64.1	-61.2
	3.8×10^{-3}	2853	1081	-64.6	-60.2
	7.6×10^{-3}	2144	1624	-69.0	-54.3
	1.1×10^{-2}	625	710	-83.9	-77.3
	1.9×10^{-2}	159	301	-92.6	-79.3
	2.7×10^{-2}	56	147	-94.0	-90.7
	3.810^{-2}	26	100	-94.3	-85.8
676	3.8×10^{-3}	2663	1009	-60.3	-56.6
	7.6×10^{-3}	1443	1093	-66.8	-65.9
	1.1×10^{-2}	1182	1343	-60.7	-67.9
	1.5×10^{-2}	1072	1623	-74.9	-67.6
	3.0×10^{-2}	485	1469	-78.9	-67.9
	4.5×10^{-2}	165	748	-85.8	-80.1
	9.1×10^{-2}	24	216	-94.6	-82.2
As-cast				-103.9	

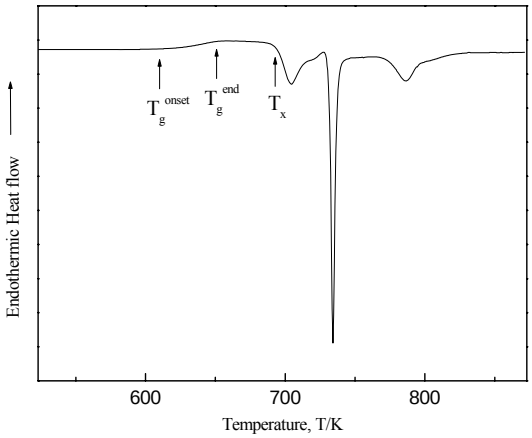

Fig.1 DSC curve of $Zr_{41.2}Ti_{13.8}Ni_{10}Cu_{12.5}Be_{22.5}$ bulk metallic glass

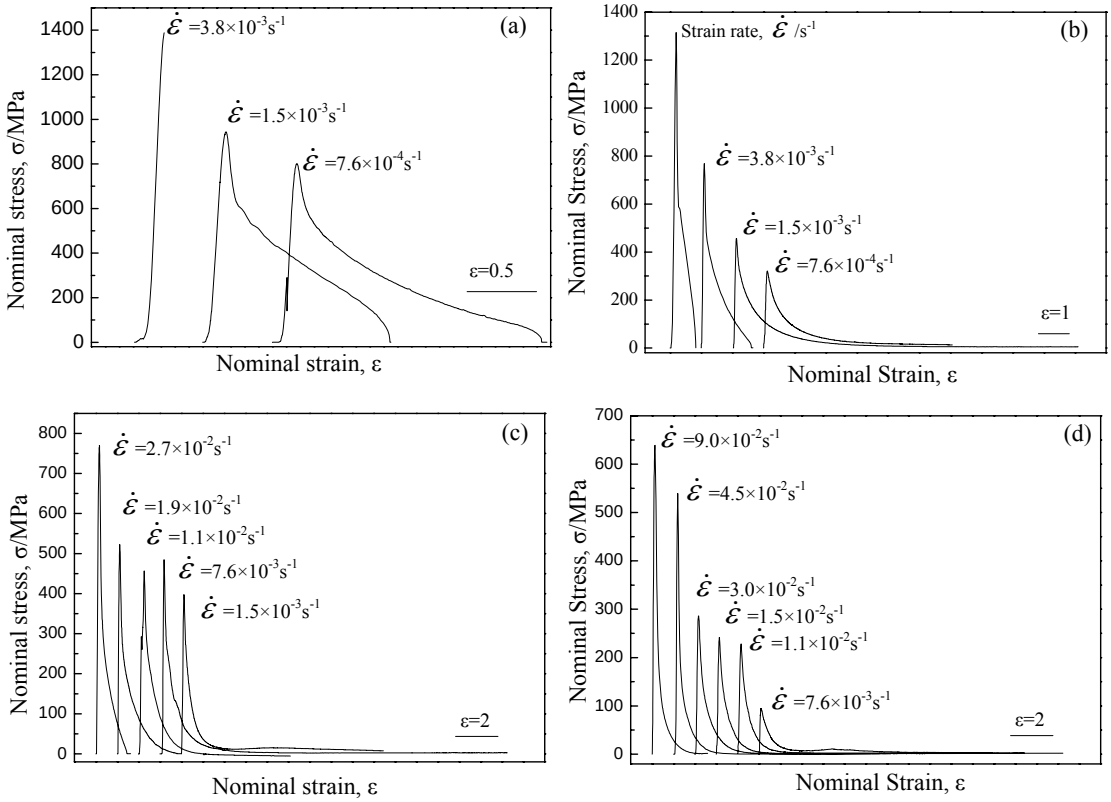

Fig.2 Nominal stress-strain curves at differential temperatures of 616K(a), 636K(b), 656K(c), 676K(d).

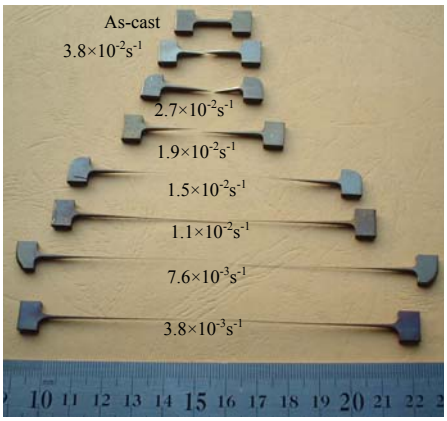

Fig.3 Photographs of the specimens which deformed at 656K and different strain-rates

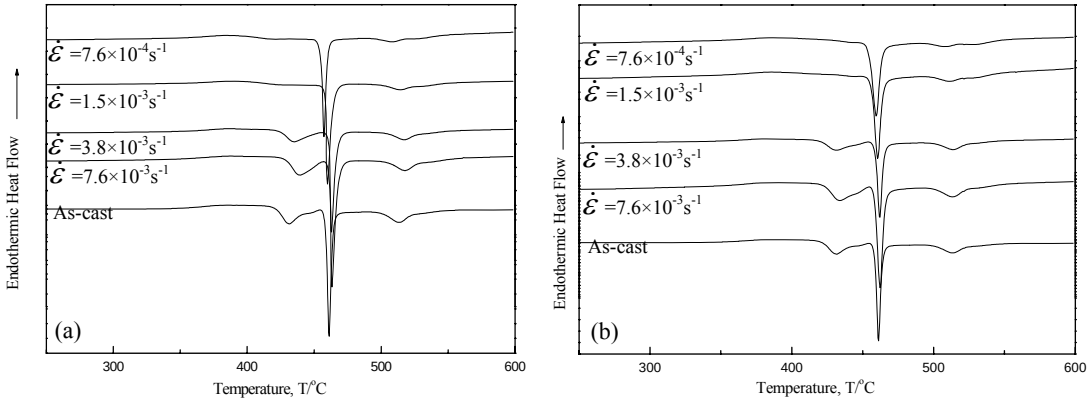

Fig.4 DSC curves for undeformed section(a) and deformed section(b) of specimens after tensile tested at 636K with differential initial strain-rates.

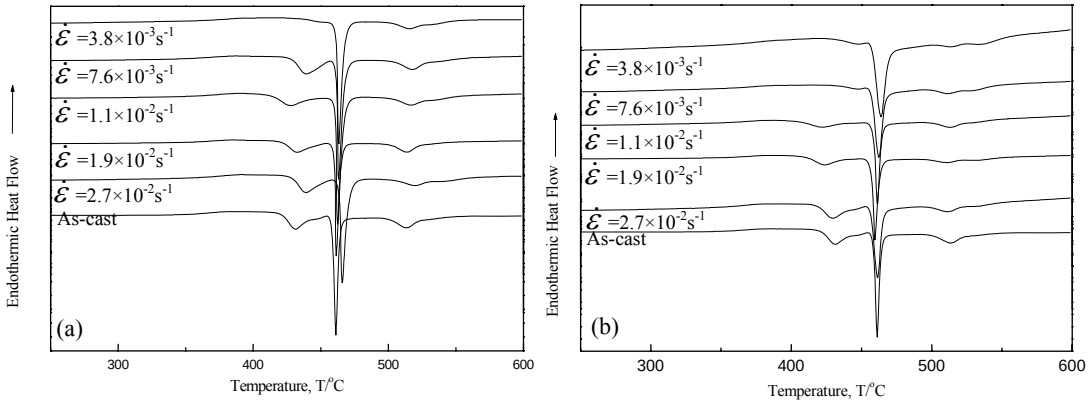

Fig.5 DSC curves for undeformed section(a) and deformed section(b) of specimens after tensile tested at 656K with differential initial strain-rates.

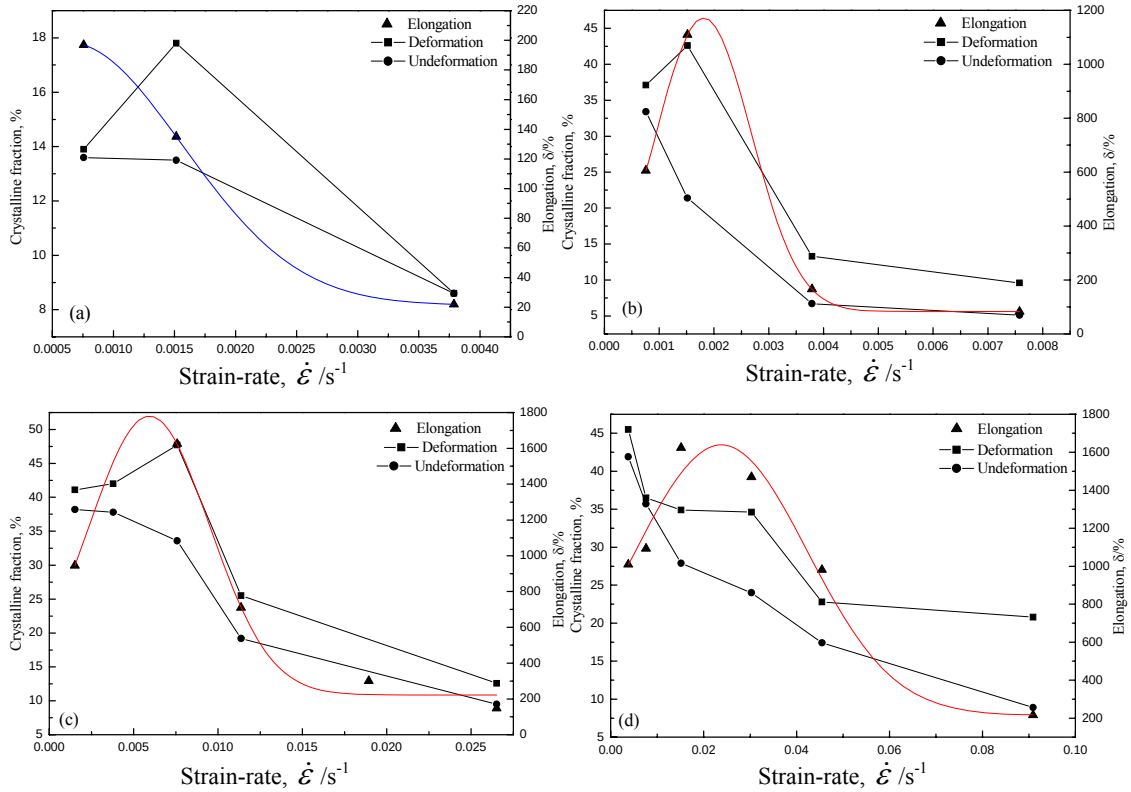

Fig.6 Crystalline volume fraction as a function of strain-rate for deformed and undeformed sections of the specimens after tensile tested at 616K(a), 636K(b), 656K(c), and 676K(d).

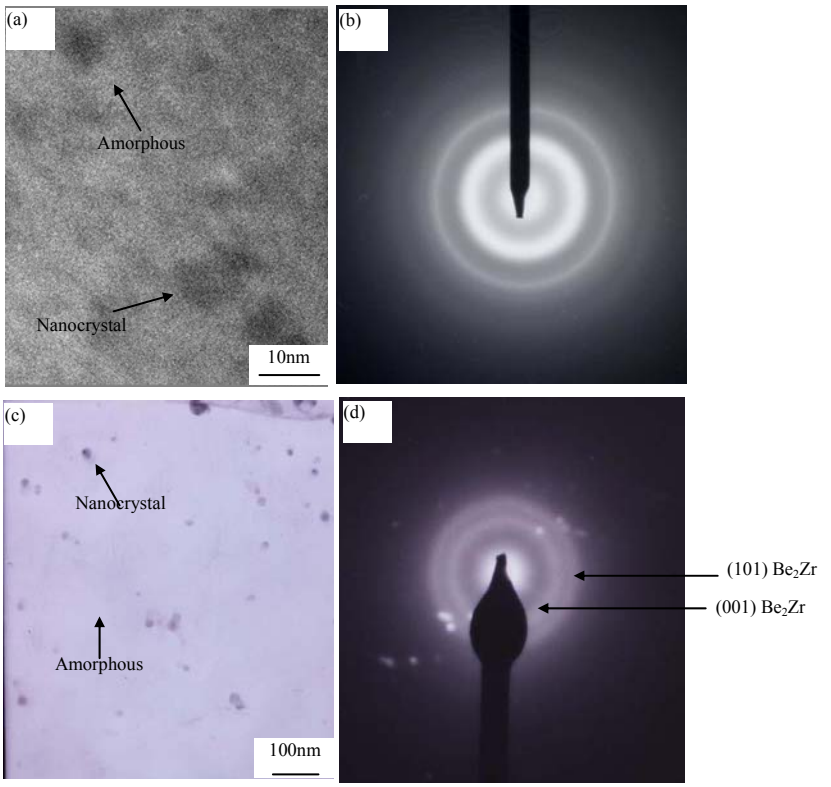

Fig.7 Bright-field TEM images and corresponding SAED patterns. (a) deformed at 636K with $7.6\times10^{-4}s^{-1}$; (b) SAED pattern corresponds to (a); (c) deformed at 656K with $7.6\times10^{-3}s^{-1}$; (d) SAED pattern corresponds to (c).